Research Square

Preprints are preliminary reports that have not undergone peer review.
They should not be considered conclusive, used to inform clinical practice,
or referenced by the media as validated information.

Effects of Plasmonic Photothermal Nanoparticles on the emission spectrum of Rh6G Dye

Mariam Kadhim Jawad
Department of Laser Physics, College of Science for Women, University of Babylon, Hillah, Iraq
Jassim Mohammed Jassim
wsci.jassem.mohamed@uobabylon.edu.iq
Department of Laser Physics, College of Science for Women, University of Babylon, Hillah, Iraq
https://orcid.org/0000-0003-3806-3675
Saddam Flayeh Haddaw
Department of Laser Physics, College of Science for Women, University of Babylon, Hillah, Iraq
Khalid Mahdi Jasim
Department of Laser Physics, College of Science for Women, University of Babylon, Hillah, Iraq
Seyedeh Mehri Hamdi
Magneto-Plasmonic Lab, Laser and Plasma Research Institute, Shahid Beheshti University, Tehran, Iran

Data Note

Keywords: Plasmoinc, Phtothermal, AuNPs, CuNPs, Rh6G dye, Emission Spectrum

Posted Date: May 26th, 2026

DOI: https://doi.org/10.21203/rs.3.rs-9796049/v1

License: This work is licensed under a Creative Commons Attribution 4.0 International License.
Read Full License

Additional Declarations: The authors declare no competing interests.

Abstract

This study investigates the influence of plasmonic photothermal gold nanoparticles (AuNPs) on the emission behavior of rhodamine 6G (Rh6G) dye. AuNPs were synthesized via pulsed laser ablation in distilled water and characterized using UV–Vis spectroscopy. The nanoparticles exhibited a distinct surface plasmon resonance (SPR) peak in the visible range, confirming their strong light absorption and scattering capability. The experimental results revealed that increasing the nanoparticle concentration and laser exposure enhanced the photothermal response, leading to higher local temperatures within the dye medium. The temperature-dependent fluorescence spectra of Rh6G showed decreased emission intensity, spectral broadening, and a slight redshift at elevated temperatures, which were attributed to increased non-radiative decay and molecular interactions. These findings demonstrate that plasmonic AuNPs effectively modulate dye emission through localized heating and plasmonic coupling, offering promising potential for tunable photothermal and random-laser applications.

1. Introduction

Gold nanoparticles (AuNPs) have emerged as promising plasmonic materials for enhancing light–matter interactions in laser systems. Their strong localized surface plasmon resonance (LSPR) effect enables significant amplification of electromagnetic fields near the nanoparticle surface, which can be effectively utilized to control and enhance the emission behavior of fluorescent dyes, such as rhodamine 6G (Rh6G) [1]. When AuNPs are dispersed in an Rh6G dye solution and excited by a Nd: YAG laser, random lasing can be achieved with distinctive spectral narrowing and intensity enhancement owing to the plasmonic coupling between the nanoparticles and dye molecules.

Rhodamine 6G is widely used as a gain medium in dye lasers because of its high fluorescence quantum yield and strong absorption around 530 nm, which matches the excitation wavelength of frequency-doubled Nd:YAG lasers. The incorporation of gold nanoparticles into the Rh6G medium further enhances its optical gain by concentrating the incident light field through localized surface plasmons, resulting in increased spontaneous and stimulated emission efficiencies [2, 3].

The performance of random lasers based on Rh6G–AuNP composites is strongly influenced by the spectral overlap between the surface plasmon resonance of the nanoparticles and the emission spectrum of the dye. This resonance overlap promotes efficient excitation energy transfer, local-field amplification, and modification of the emission characteristics [4, 5]. Additionally, factors such as nanoparticle size, shape, concentration, and distance from dye molecules play crucial roles in determining the degree of plasmonic enhancement.

Surface plasmons, which are collective oscillations of conduction electrons at the metal–dielectric interface excited by electromagnetic radiation, govern the optical response of Au nanoparticles [6, 7]. Their excitation leads to enhanced scattering and absorption, as well as efficient photothermal conversion. In random laser systems, moderate concentrations of AuNPs improve the feedback and optical gain in the weakly scattering regime, whereas excessively high concentrations can induce non-

radiative losses and fluorescence quenching [8]. Therefore, optimizing the plasmonic–dye coupling parameters is essential for achieving efficient random lasing and tunable emission properties in Rh6G–AuNP systems [9].

2. Preparation of Pure Metal Nanoparticles

We synthesized gold (Au)) nanoparticles using the laser ablation in liquid (LAL) technique, a chemical-free method that enables the production of clean and stable colloids. In this process, we placed a high-purity metal target (Au) at the bottom of a quartz container filled with 10 ml of deionized water containing polyvinylpyrrolidone (PVP). We prepared the polymer matrix by dissolving PVP in deionized water at a weight ratio of 1:100 (PVP: water).

The mixture was continuously stirred at room temperature until the PVP was completely dissolved, resulting in a clear, homogeneous solution. We chose PVP for its excellent water solubility, optical clarity, and known ability to stabilize dispersed nanoparticles, reducing their agglomeration and enhancing their colloidal stability.

We used a Q-switched Nd: YAG laser operating at a wavelength of 1064 nm, a pulse energy of 100 mJ, and a repetition rate of 10 Hz. We focused the laser beam onto the target surface using a convex lens (focal length of 25 cm) and performed ablation for 4 minutes (approximately 2,400 pulses), yielding a colloidal solution of nanoparticles. The intense interaction between the laser and the target led to rapid heating, melting, and evaporation of the target, forming a plasma plume. As the column cooled in the liquid, the atoms and clusters condensed into nanoparticles. This method allows precise control of particle size and composition without the need for surfactants or reducing agents. The resulting colloids exhibited a distinct color depending on the metal type, as shown in figure (1). AuNPs exhibited a wine-red color due to their surface plasmon resonance (SPR) bands,

3. Experimental set-up of the Photothermal effect

We studied the photothermal effect in dye-based random laser systems using two rhodamine 6G (R6G) liquid samples at different concentrations. The first and second solutions were 1×10^{-5} M and 1×10^{-4} M, respectively. Both solutions were transferred into quartz cuvettes with an optical path length of 1 cm. Figures (2) schematically illustrates the experimental setup used to study the photothermal effect. We used an Nd: YAG laser operating at a wavelength of 532 nm, while an 810 nm diode laser was used simultaneously to induce photothermal heating in the solution. The laser beam was passed through a neutral density attenuator to control the incident energy before reaching the sample. The photothermal effect was induced directly by 810 nm diode laser radiation, resulting in the localized heating of the dye solution. We monitored the temperature changes and thermal responses in real time using thermocouples. Fluorescent emissions were collected at an angle of 90° to the incident laser using an optical fiber connected to a high-resolution spectrometer (0.3 nm resolution).

4. Results and Discussions

4.1 Absorption spectra of Au Nanoparticles:

We investigated the light absorption properties of gold (Au)) nanoparticles due to their prominent surface plasmon resonance (SPR) properties in the visible region. These nanoparticles exhibit strong light-matter interaction, which depends on size, shape, and environment. For gold nanoparticles, we observed a characteristic SPR absorption peak typically around 525 nm, as shown in Figure (3). This is attributed to the collective oscillation of conduction electrons on the nanoparticle surface in resonance with the incident light. In contrast, copper nanoparticles exhibited a broader and slightly redshifted SPR peak in the 690 nm range, due to higher damping losses and oxidation susceptibility.

4.2 Morphology Characterizations:

The structural characterization of the synthesized nanoparticles was conducted using Field Emission Scanning Electron Microscopy (FE-SEM). The (FE-SEM) image and Particle size distribution histograms for Au nanoparticles are shown in figure (4). We analyzed the particle size distribution plots of the synthesized Au nanoparticles to evaluate the uniformity and dispersion of particle sizes. Nanoparticles (Au NPs) exhibit a well-defined cubic morphology, which is in agreement with the characteristic crystalline structure of gold [10]. This cubic geometry reflects the intrinsic growth behavior of Au NPs produced under precisely controlled laser ablation conditions.

4.3 Impact of laser radiation exposure duration and Nanoparticle Concentration on dye temperature

We observed a consistent trend in all samples, where the dye temperature gradually increased with the duration of laser irradiation, as shown in Figure (5). At shorter exposure times (30–150 s), the temperature increase was nearly linear, reflecting continuous heat deposition through photon absorption and non-radiative relaxation. With further exposure (up to 420 s), the rate of temperature increase began to slow down, indicating the onset of thermal equilibrium between heat generation within the dye medium and heat dissipation into the surrounding interment. The figure also shows a direct relationship between the number of laser pulses and the magnitude of the temperature increase.

For the sample prepared with 800 pulses, the maximum recorded temperature increase (ΔT) after 420 s was 5.1°C, reaching a final temperature of ~ 35.1°C. Increasing the pulse number to 1000 enhanced the heating effect, where the dye temperature increased to 36.6°C (ΔT = 6.6°C). The most pronounced effect was observed for the 2000-pulse sample, in which the dye reached 38.8°C with a maximum ΔT of 8°C after 420 s of exposure. This behavior confirms that a higher number of laser pulses results in a stronger cumulative energy deposition, thereby intensifying the photothermal effect on the dye solution [10].

4.4 Heat generated and dissipation in gold nanoparticles under pulsed laser irradiation: a numerical simulation

Using COMSOL Multiphysics software, we conducted a thorough numerical simulation to examine the processes of heat generation and dissipation in gold (Au). A nanosecond pulsed laser with a central wavelength of 532 nm, temporal breadth of 4 ns, and pulse repetition rate of 10 Hz served as the laser source in this simulation [12, 13]. Following laser pulse irradiation, the simulation results displayed in Figure (6) unequivocally demonstrate a significant rise in the nanoparticles' temperature. Because PVP and water have different thermal coefficients, the resultant graphs show that when the nanoparticles were added to the PVP solution, their temperature increased more.

4.5 Effect of temperature on the emission spectrum of Rh6G Dye:

After preparing Rh6G dye solutions at different concentrations and carefully analyzing their absorption spectra, we captured the corresponding fluorescence emission spectra using a fluorescence spectrometer, as shown in Figure (7).

Our results indicate that the fluorescence intensity initially increased with increasing dye concentration, reaching a peak at a concentration of 5×10^{-4} M. Beyond this concentration, we observed a decrease in fluorescence intensity, which was attributed to concentration-dependent quenching effects, such as reabsorption and dye-to-dye interactions.

Based on these observations, we determined the 5×10^{-5} M concentration as the optimal value for achieving the strongest emission and chose it as the most suitable concentration for the active gain medium in subsequent random laser experiments. In addition, a slight redshift in the emission peak was observed with increasing dye concentration. Specifically, the emission maximum shifted from 551 nm at 5×10^{-6} M to 553.5 nm at 5×10^{-4} M, indicating that higher concentrations resulted in a slight energy loss during fluorescence, possibly due to increased molecular interactions or reabsorption [15].

We also examined the fluorescence spectra of Rh6G dye solutions containing gold nanoparticles (AuNPs) at various temperatures ranging from 25 to 45°C. Figures (8) presents a comparison of two samples composed of Rh6G–AuNPs mixtures with different dye concentrations. The experimental observations clearly show that the temperature and the presence of AuNPs jointly affect the fluorescence behavior of the system.

As the temperature increased, a gradual decrease in the fluorescence intensity, broadening of the spectral width, and slight redshift of the emission peak were observed. These variations can be attributed to both the thermal effects and plasmonic interactions induced by the AuNPs. The localized surface plasmon resonance (LSPR) of nanoparticles enhances the local electromagnetic field, promoting radiative transitions at lower temperatures. However, at elevated temperatures, the

photothermal effect of AuNPs leads to increased non-radiative relaxation pathways and dye interactions, resulting in fluorescence quenching and spectral broadening.

Quantitatively, for the Rh6G–AuNP solution with a concentration of 1×10^{-5} M, the peak intensity decreased from approximately 21,200 a.u. at 25°C to approximately 14,200 a.u. at 45°C, while the FWHM increased from 39.5 nm to 40.4 nm. Similarly, for the 1×10^{-4} M sample, the peak intensity decreased from 24,000 a.u. to 17,500 a.u., accompanied by an increase in the FWHM from 41.0 nm to 42.4 nm.

Conclusions

The UV–Vis absorption spectra confirmed a strong surface plasmon resonance (SPR) peak in the visible region, indicating efficient light–matter interactions. Experimental measurements demonstrated that both the laser exposure duration and number of ablation pulses significantly affected the photothermal response of the dye solution. The temperature of the Rh6G solution increased progressively with exposure time, reaching a maximum rise (ΔT) of 8°C after 420 s for the 2000-pulse sample, compared with 5.1°C for the 800 pulses. This clearly demonstrates that increasing the laser pulse energy enhances cumulative heating through stronger plasmonic absorption.

Numerical simulations using COMSOL Multiphysics further supported these findings, revealing that the AuNPs exhibited efficient light-to-heat conversion and faster cooling dynamics than the CuNPs. When dispersed in water or PVP, the simulated temperature increase of the AuNPs increased sharply with the pulse energy (1–5 mJ), confirming their superior photothermal efficiency and rapid thermal diffusion compared to those of copper.

Fluorescence spectral analysis of Rh6G at various concentrations and temperatures provided additional evidence of the thermal influence on optical emission. The optimal emission intensity was achieved at a concentration of 5×10^{-5} M, beyond which fluorescence quenching was observed due to reabsorption and molecular aggregation. Temperature-dependent fluorescence measurements showed that increasing the temperature from 25 to 45°C led to a decrease in peak intensityfrom 21,200 a.u. to 14,200 a.u. for the 1×10^{-5} M sampleand a corresponding broadening of the FWHM from 39.5 nm to 40.4 nm, accompanied by a slight redshift of the emission peak.

These combined experimental and simulation results confirm that the localized heating induced by AuNPs strongly modulates the fluorescence efficiency and spectral characteristics of the Rh6G dye. The coupling between surface plasmon resonance and dye emission enhances light amplification at optimal nanoparticle concentrations, whereas excessive heating leads to fluorescence quenching. Overall, this study demonstrates that plasmonic AuNPs serve as efficient photothermal agents capable of tuning the emission intensity, linewidth, and spectral position of Rh6G, offering valuable potential for temperature-controlled random lasers, photonic sensors, and nanophotothermal devices.

Declarations

Contributions author: J. M. Jassim provided supervision and methods, including writing, review, editing, and proofreading; S. F. Haddawi provided review and editing; The original draft was written by Maryam Kadhim Jawad; Khalid Mahdi Jassim: The experiment's setup and findings, S. M. Hamidi oversees the project.

Declaration of Competing Interest :

There is no any conflict interest .

Funding source:

There was no funding for this study.

Data availability statement:

The authors declare no conflict of interest.

References

1. Yu H, Peng Y, Yang Y, Li ZY (2019) Plasmon-enhanced light–matter interactions and applications. npj Comput Mater 5(1):45
2. Hartland GV (2011) Optical studies of dynamics in noble metal nanostructures. Chem Rev 111(6):3858–3887
3. Jawad MH, Abdulameer MR (2025) Spectral analysis of brass plasma generated by a Nd: YAQ laser at λ = 1064 nm. Russ Phys J, 1–9
4. Ismail WZW, Dawes JM (2022) Synthesis and characterization of silver-gold bimetallic nanoparticles for random lasing. Nanomaterials 12(4):607
5. Ismail WZW, Vo TP, Goldys EM, Dawes JM (2015) Plasmonic enhancement of Rhodamine dye random lasers. Laser Phys 25(8):085001
6. Debela S, Mesfin B, Senbeta T (2019) Surface plasmon resonances in ellipsoidal bimetallic nanoparticles. Photonics Nanostructures-Fundamentals Appl 33:48–54
7. 4-Brongersma ML, Kik PG (eds) (2007) Surface plasmon nanophotonics, vol 131. Springer
8. 5-Yeshchenko OA, Kutsevol NV, Naumenko AP (2016) Light-induced heating of gold nanoparticles in colloidal solution: dependence on detuning from surface plasmon resonance. Plasmonics 11:345–350
9. Dong L, Ye F, Hu J, Popov S, Friberg AT, Muhammed M (2011) Fluorescence quenching and photobleaching in Au/Rh6G nanoassemblies: impact of competition between radiative and non-radiative decay. J Eur Opt Society-Rapid publications 6:11019

10. Oliveira AEF et al (2023) Gold nanoparticles: a didactic step-by-step of the synthesis using the Turkevich method, mechanisms, and characterizations. Analytica 4(2):250–263
11. Kumar BR, Basheer NS, Kurian A, George SD (2013) Thermal-Lens study on the distance-dependent energy transfer from Rhodamine 6G to gold Nanoparticles. Int J Thermophys 34(10):1982–1992
12. Tran M, DePenning R, Turner M, Padalkar S (2016) Effect of citrate ratio and temperature on gold nanoparticle size and morphology. Mater Res Express 3(10):105027
13. Haddawi MF, Jassim JM, Roostaei N, Hamidi SM (2023) Red and green plasmonic-induced random laser in two-dimensional square array onto glass substrate. Optik 283:170929
14. Jawad MK, Jassim JM, Haddawi SF, Hamidi SM (2025) Temperature effects on the conversion coupling efficiency in dye-based plasmonic random laser gain media. J Theoretical Appl Phys 19(1):1–6
15. Al-Sultani MMM (2019) Study the effects for both diode laser and silica nanoparticles in the optical properties of the dental fillings. Res J Pharm Technol 12(11):5355–5360

Figures



Figure 1

Color Appearance of Prepared AuNPs

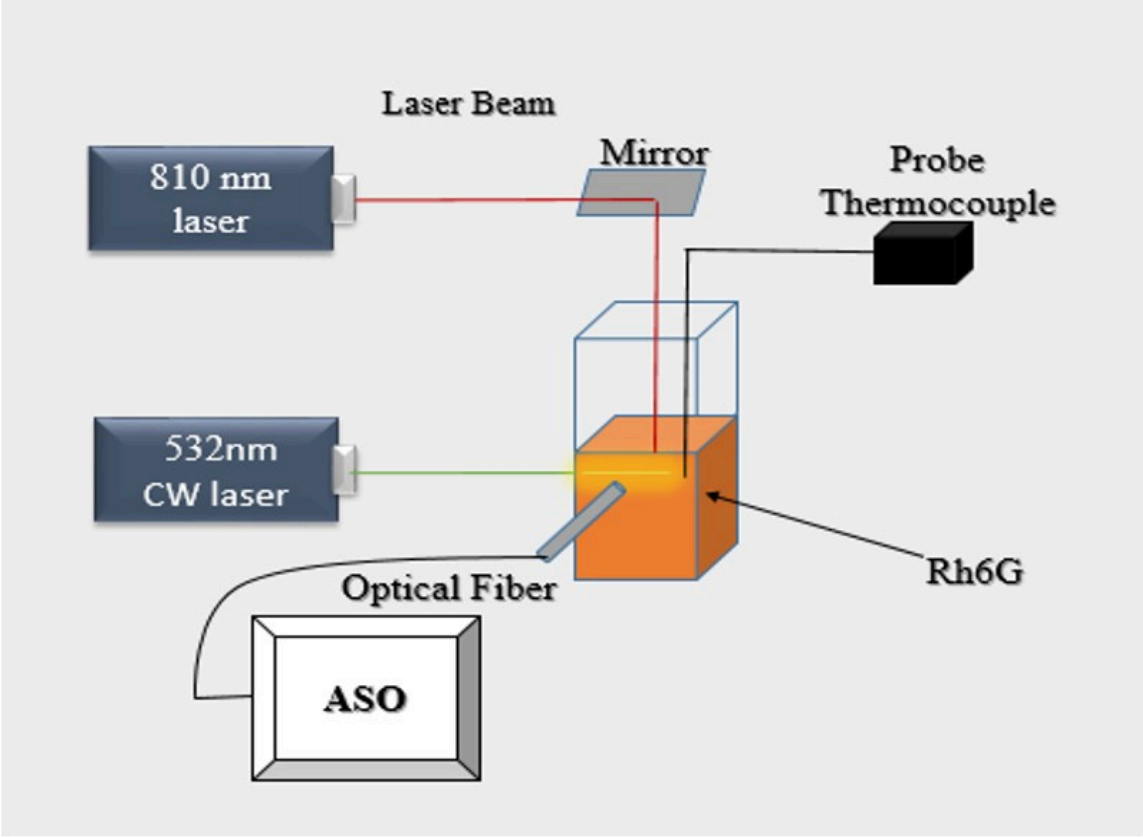


Figure 2

Schematic of the photothermal experimental setup.

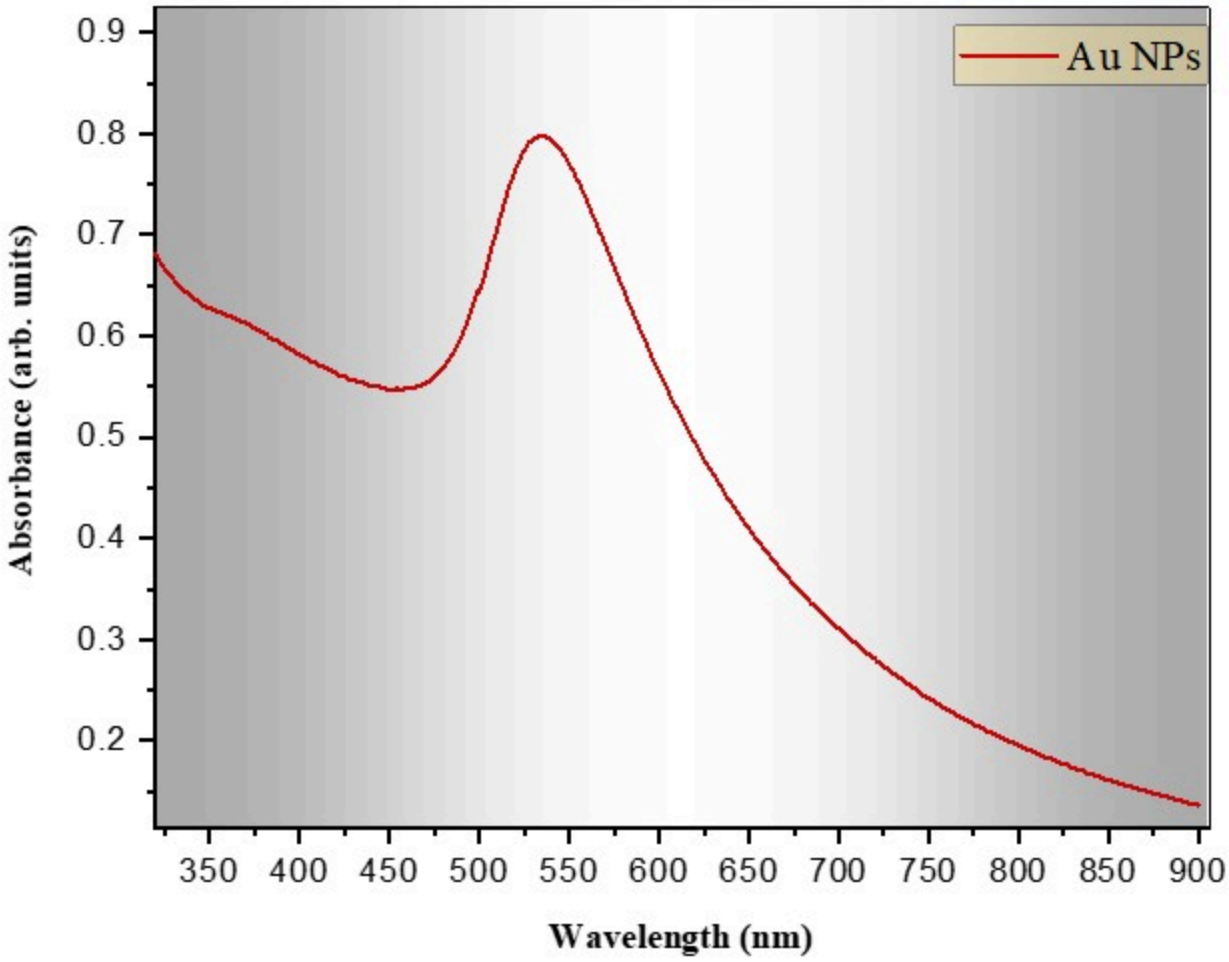


Figure 3

Absorption spectra of Au NPs.

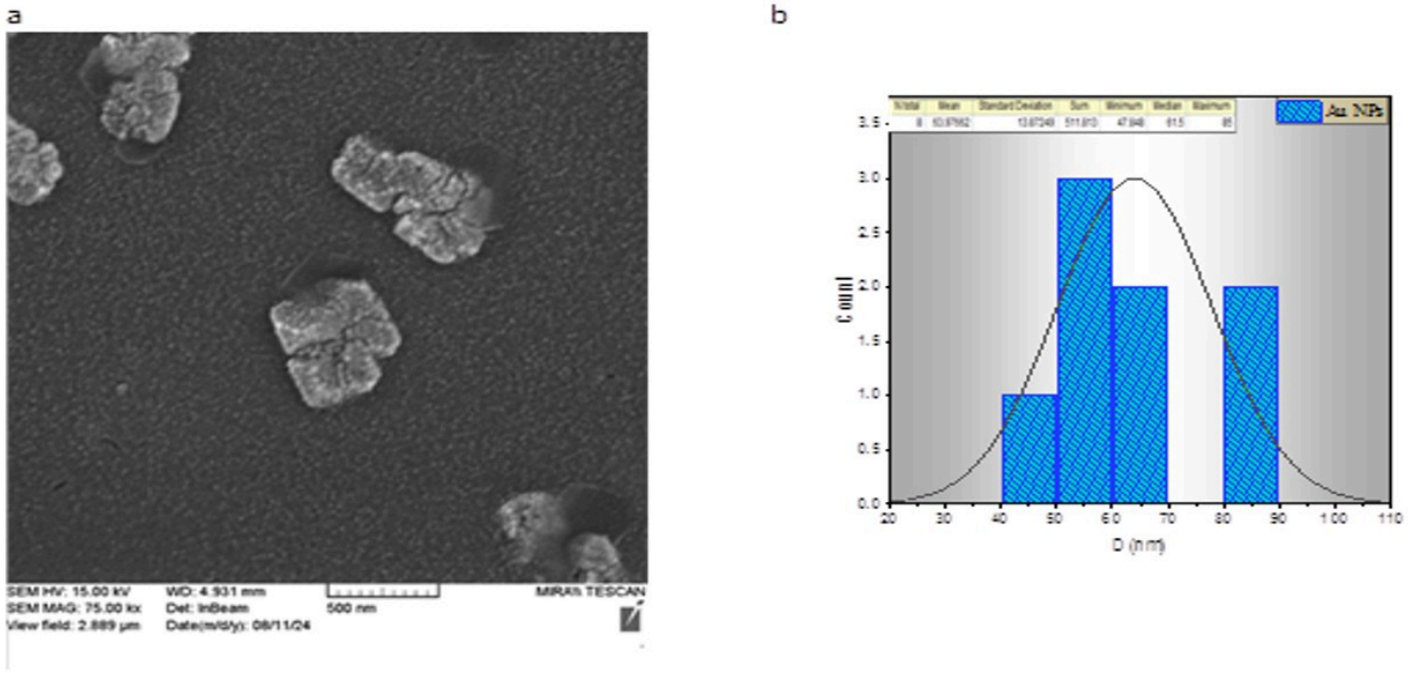


Figure 4

(a) FE-SEM image and (b) Particle size distribution histograms for Au NPs.

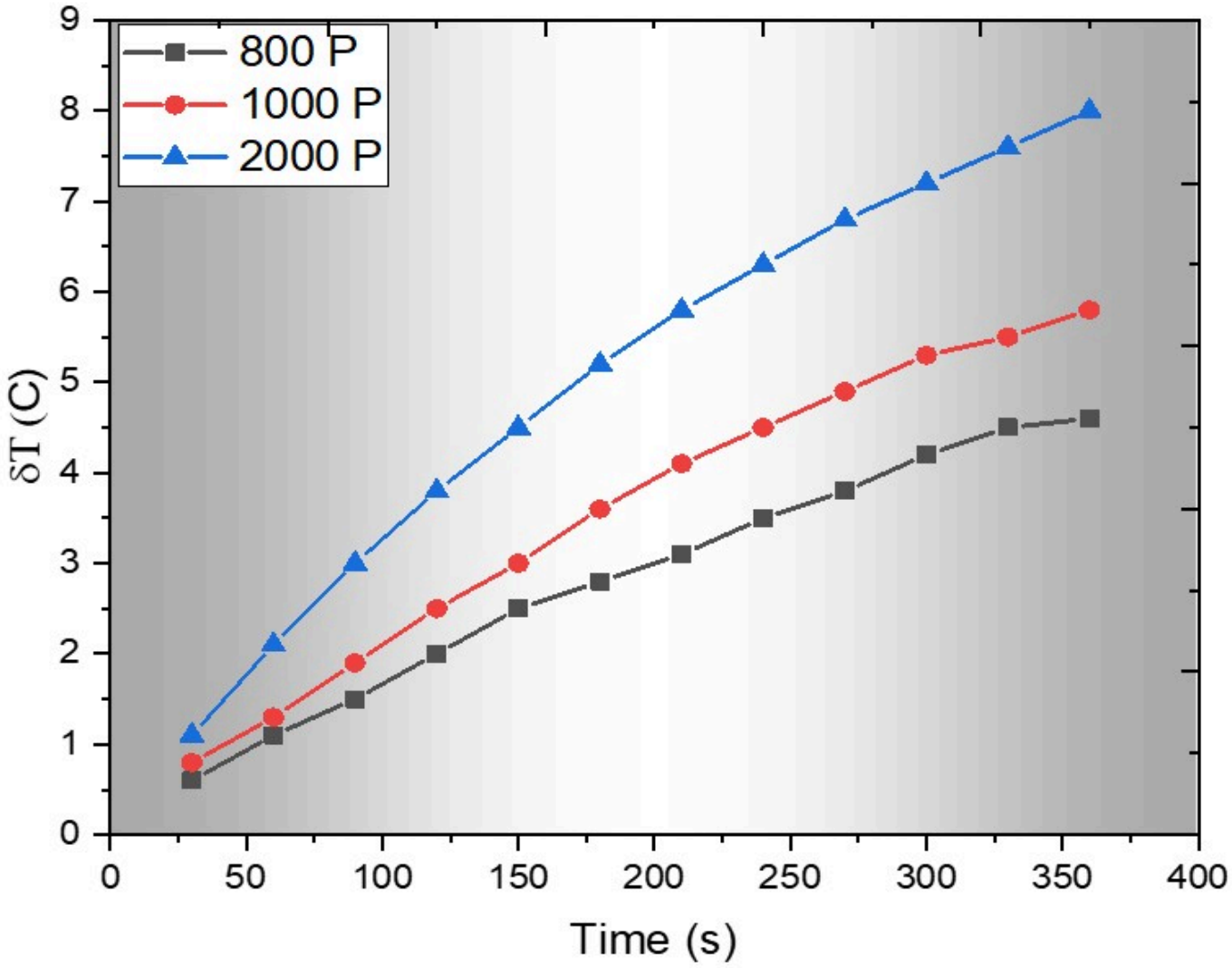


Figure 5

Comparison of dye temperature variation with exposure time for NPs at different laser pulses.

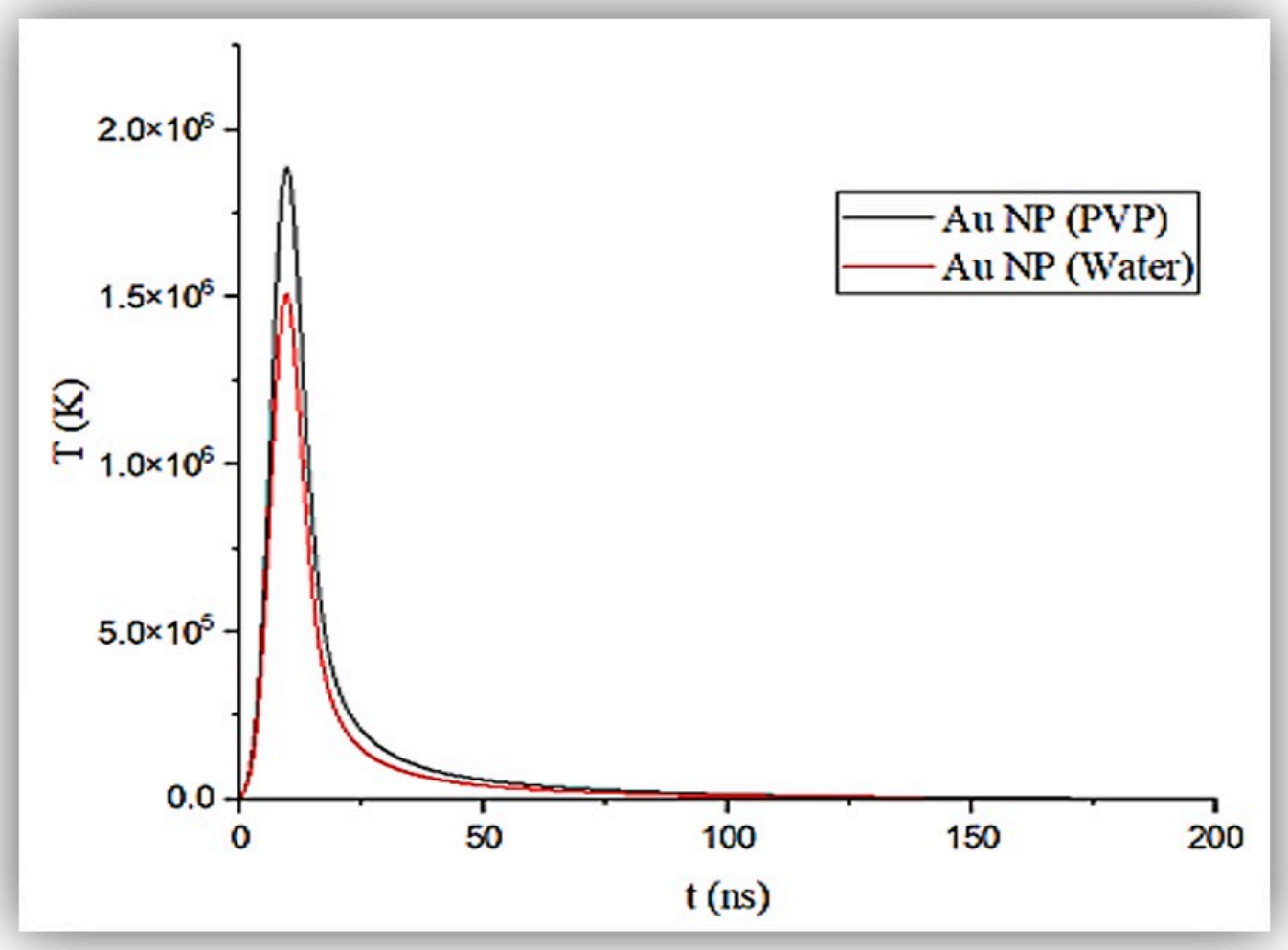


Figure 6

Au NPs in water and PVP simulation results.

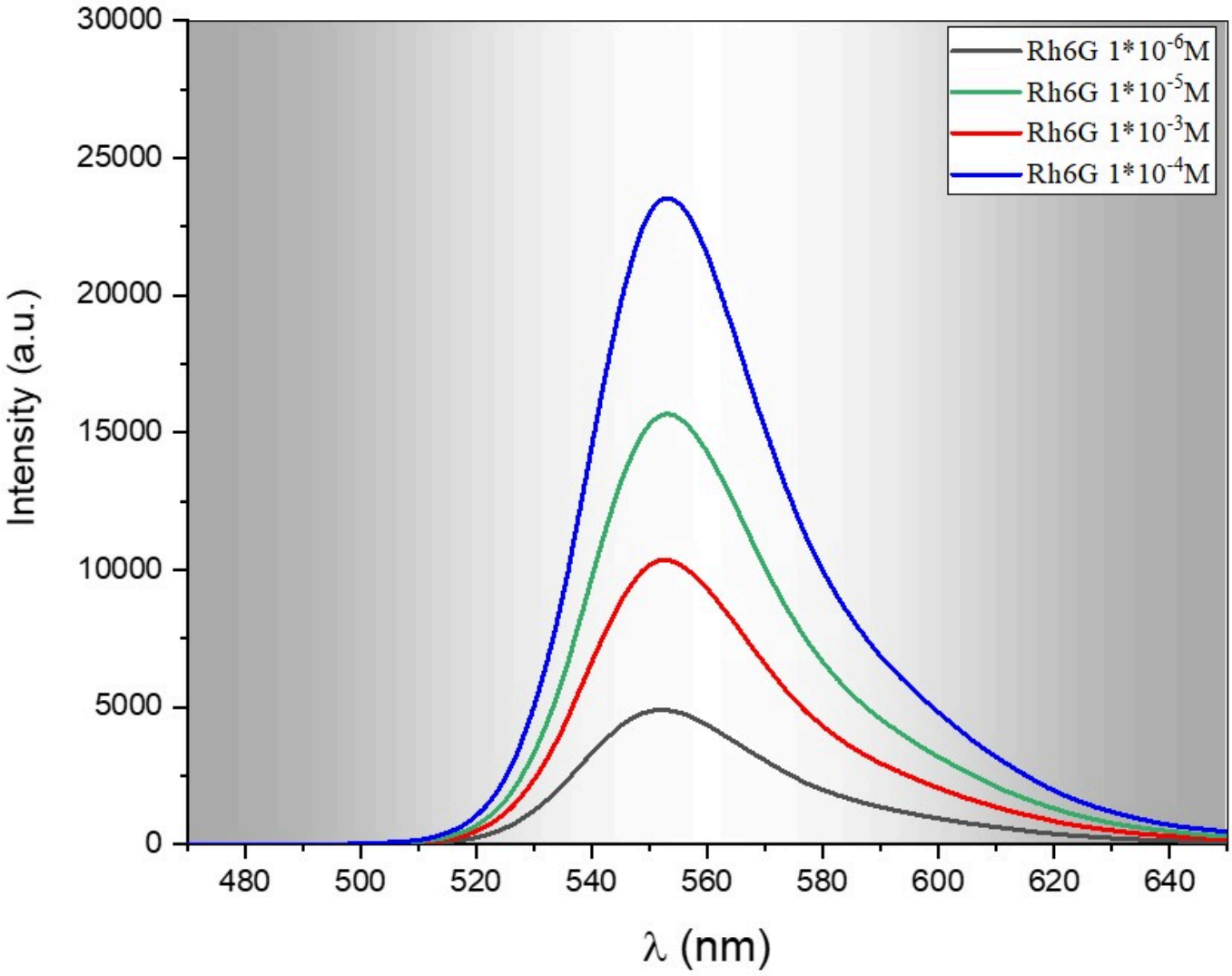


Figure 7

Fluorescence spectrum of Rh6G at room temperature and different concentrations.

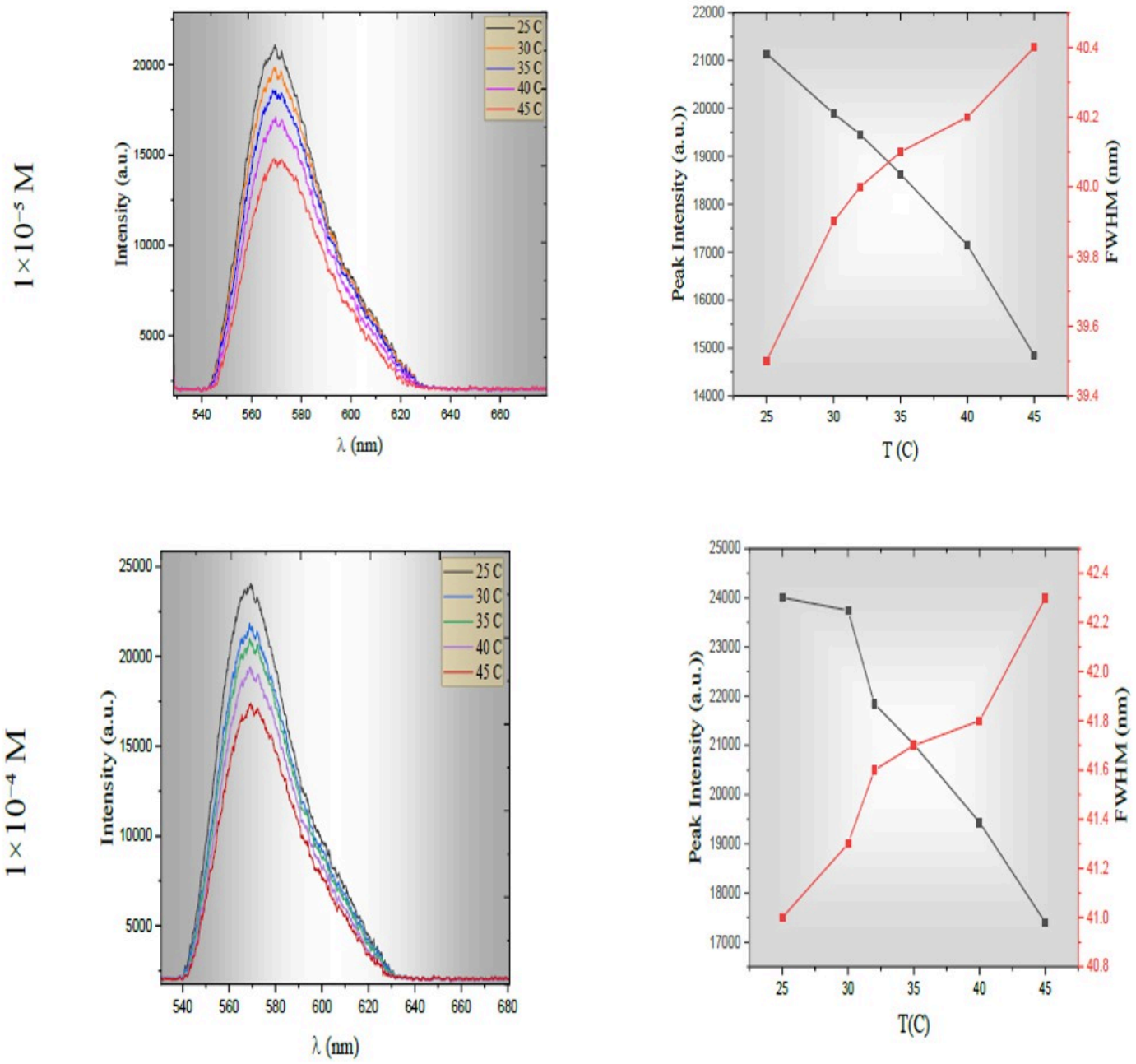


Figure 8

Fluorescence spectra of Rh6G dry film under different temperature conditions for different concentrations.